www.sciencetranslationalmedicine.org/cgi/content/full/5/167/167ra5/DC1

Supplementary Materials for

Targeting the JMJD2 Histone Demethylases to Epigenetically Control Herpesvirus Infection and Reactivation from Latency

Yu Liang, Jodi L. Vogel, Jesse H. Arbuckle, Ganesha Rai, Ajit Jadhav, Anton Simeonov, David J. Maloney, Thomas M. Kristie*

*To whom correspondence should be addressed. E-mail: thomas_kristie@nih.gov

Published 9 January 2013, *Sci. Transl. Med.* **5**, 167ra5 (2013)
DOI: 10.1126/scitranslmed.3005145

The PDF file includes:

Materials and Methods
Fig. S1. Depletion of JMJD2 members resulted in decreased HSV-1 IE mRNAs.
Fig. S2. ML324-mediated inhibition of HSV lytic infection and reactivation from latency.
Fig. S3. Selective induction of JMJD2D transcription upon infection with hCMV.
Fig. S4. Levels of JMJD2 mRNAs in selected tissues and cell types.
Fig. S5. Structure and characteristics of ML324.
Table S1. Antibodies and primers.

Supplementary Materials

Materials and Methods

Construction and selection of cell lines expressing siRNA-resistant JMJD2 constructs

siRNA-resistant JMJD2 expression constructs were produced by site directed mutagenesis using the Quik Change Site Directed Mutagenesis Kit (Stratagene). HeLa cells were transfected with control pcDNA3-lacZ or pcDNA3-siRNA-resistant JMJD2 expression constructs. Forty-eight hrs post transfection, cells were selected with 800 μg/ml G418 until the establishment of resistant colonies. G418-resistant cells expressing the siRNA-resistant JMJD2 proteins were depleted for the homologous endogenous JMJD2 by siRNA transfection. mRNA or protein levels of viral and cellular genes were measured by qRT-PCR and/or Western blot.

ChIP Assays

Lysates of formaldehyde crosslinked HeLa cell nuclei were sonicated using a Branson digital Sonifier 450 (25% amplitude, 8 cycles) to obtain DNA fragments averaging 500-750 bp. Chromatin from ~7-8 x 10^5 cells were subjected to immunoprecipitation with the indicated antiseras (table S1). Immunoprecipitates were washed, eluted, and crosslinking was reversed as previously described (16, 18, 49). Immunoprecipitated DNAs were analyzed, in triplicate, by qPCR using Roche FastStart Universal SYBER Green Master (04913914001) on an ABI PRISM 7900HT (ABI SDS 2.3 software) or Eppendorf RealPlex4 Mastercycler (Realplex 2.2 software). For JMJD2, HCF-1, and RNAPII ChIPs, the percent bound-signals of negative control viral regions (UL32 or UL47 ORFs) were subtracted from the percent bound-signals of experimental regions.

Coimmunoprecipitations

293F cells were transfected with constructs expressing HA-tagged JMJD2 proteins or were cotransfected with a construct expressing V5-tagged HCF-1. Nuclear extracts of transfected

cells were incubated with anti-V5 in binding buffer [50 mM Tris pH 7.5, 150 mM NaCl, 0.1% NP-40, 5% Glycerol, Complete protease inhibitor (Roche)] for 1 hr at 4°C. Immunoprecipitates were washed expensively with binding buffer, eluted in SDS sample buffer, and resolved in 4-20% Tris-Glycine gels. Western Blots of resolved extracts and immunoprecipitates were probed with an anti-HA HRP conjugate, developed with Pierce SuperSignal West Dura, and quantitated using a Kodak 4000MM Image Station.

Ganglia Immunofluorescence

HSV-1 latently infected mouse trigeminal ganglia were explanted and cultured with DMEM-10% FBS in the presence or absence of the indicated compound for 48 hrs. Ganglia were then fixed with 4% paraformaldehyde for 12 hrs, washed in PBS/70% EtOH, and embedded in paraffin. Sections were de-paraffined with Xylene and rehydrated in a series of Ethanol-H_2O solutions. For antigen retrieval, sections were boiled in 0.01M Citric Acid (pH6.0) for 10min, cooled to 48°C, and equilibrated in PBS. Sections were costained with anti-UL29 sera (gift of W. Ruyechan, SUNY Buffalo) and anti-neurofilament 200 (Sigma, # N0142, 1:200) followed by Donkey anti-mouse IgG-FITC (Jackson ImmunoResearch, #715-095-150) and Donkey anti-Rabbit IgG-TRITC (Jackson ImmunoResearch, #711-025-152). Sections were visualized using a Leica TCS SF5 confocal microscope.

Statistical Analyses

Individual statistical comparisons were made using paired-two tailed t test, unpaired two-tailed t test, Wilcoxon paired signed rank tests with a statistical significance of <0.05 (Prism V5.0a). Multiple sample comparisons were done using One-way or Two-way ANOVA followed by Dunnett or Tukey post hoc tests. Details are as follows:

Figure 3A: Two-way ANOVA with Dunnett post hoc tests; viral (ICP27 ICP4) vs. GAPDH at each DMOG concentration. The levels of both viral mRNAs were significantly different from that of the control GAPDH at DMOG concentrations 0.5, 0.75, 1.25, and 1.5 mM [$p < 0.0001$].

Figure 3B: One-way ANOVA with Dunnett post hoc test; DMSO vs. DMOG. Viral yields were significantly different from control DMSO at 1.5, 2.0, and 2.5 mM DMOG [$p < 0.0001$].

Figure 3D: Wilcoxon matched-pairs signed rank test; DMSO vs. DMOG, $p = 0.0001$, $n = 20$; DMSO vs. TCP, $p = 0.0156$, $n = 7$.

Figure 3E: Paired two-tailed t test, ICP4 mRNA levels ACV vs. DMOG, $p = 0.0015$; ICP27 mRNA levels, $p < 0.0001$; $n = 4$.

Figure 4A: Two-way ANOVA with Tukey post hoc test; viral (ICP27, ICP4, ICP22) vs. controls (S15, Sp1, TBP) at each ML324 concentration. The levels of viral mRNAs were significantly different from the levels of the controls at ML324 concentrations 10, 25, and 50 μM [$p < 0.0001$].

Figure 4B: One-way ANOVA with Dunnett post hoc test; DMSO vs. ML324. Viral yields were significantly different from control DMSO at 5, 10, 25, and 50 μM ML324 [$p < 0.004$].

Figure 4C: Two-way ANOVA with Tukey post hoc test; viral (ICP4, ICP22, IPC27) vs. control (S15, TBP). Viral mRNA levels were significantly different from the levels of the controls at 0.1, 1.0, and 10.0 MOI infection [$p < 0.0001$].

Figure 4D: Two-way ANOVA with Tukey post hoc test; DMSO vs. ACV; DMSO vs. ML324; ACV vs. ML324. ACV and ML324 viral yields were significantly different from control DMSO at 0.1, 1.0, and 10.0 MOI infection [$p < 0.0001$]. ACV and ML324 viral yields were not significantly different from one another [$p = 0.7949$ (MOI 0.1), 0.9995 (MOI 1.0), 0.3425 (MOI 10.0)].

Figure 4H: Wilcoxon matched-pairs signed rank test; DMSO vs. DMOG, $p = 0.0015$ $n = 12$; DMSO vs. ML324, $p < 0.0001$, $n = 20$.

Figure 4I: Two-tailed T test; ACV clusters vs. ML324 clusters, $p = 0.0009$, $n = 48$; ACV single vs ML324 single, $p = 0.0003$, $n = 48$; DMSO singles vs. ML324 singles, $p = 0.0002$, $n = 48$.

Figure 5E: Two-way ANOVA with Dunnett's post hoc test; DMSO vs. viral (UL37, IE72, US3) at each TCP concentration. Viral mRNA levels were significantly different from the levels of

control DMSO at each concentration [0.2 mM, $p < 0.002$; 0.4 mM, $p < 0.0001$; 0.8 mM, $p < 0.0001$; 1.5 mM, $p < 0.0001$].

Figure 5F: Two-way ANOVA with Dunnett's post hoc test; DMSO vs. viral (UL37, IE72) at each DMOG concentration. Viral mRNA levels were significantly different from the levels of control DMSO at each DMOG concentration [0.5, 0.75, 1.0, 1.25, 1.5 mM; $p < 0.0001$].

Figure 5G: Two-way ANOVA with Tukey's post hoc test; viral (IE72, US3) vs. control (S15, TBP). Ratios of viral mRNA levels were significantly different from ratios of control mRNA levels [$p < 0.0001$].

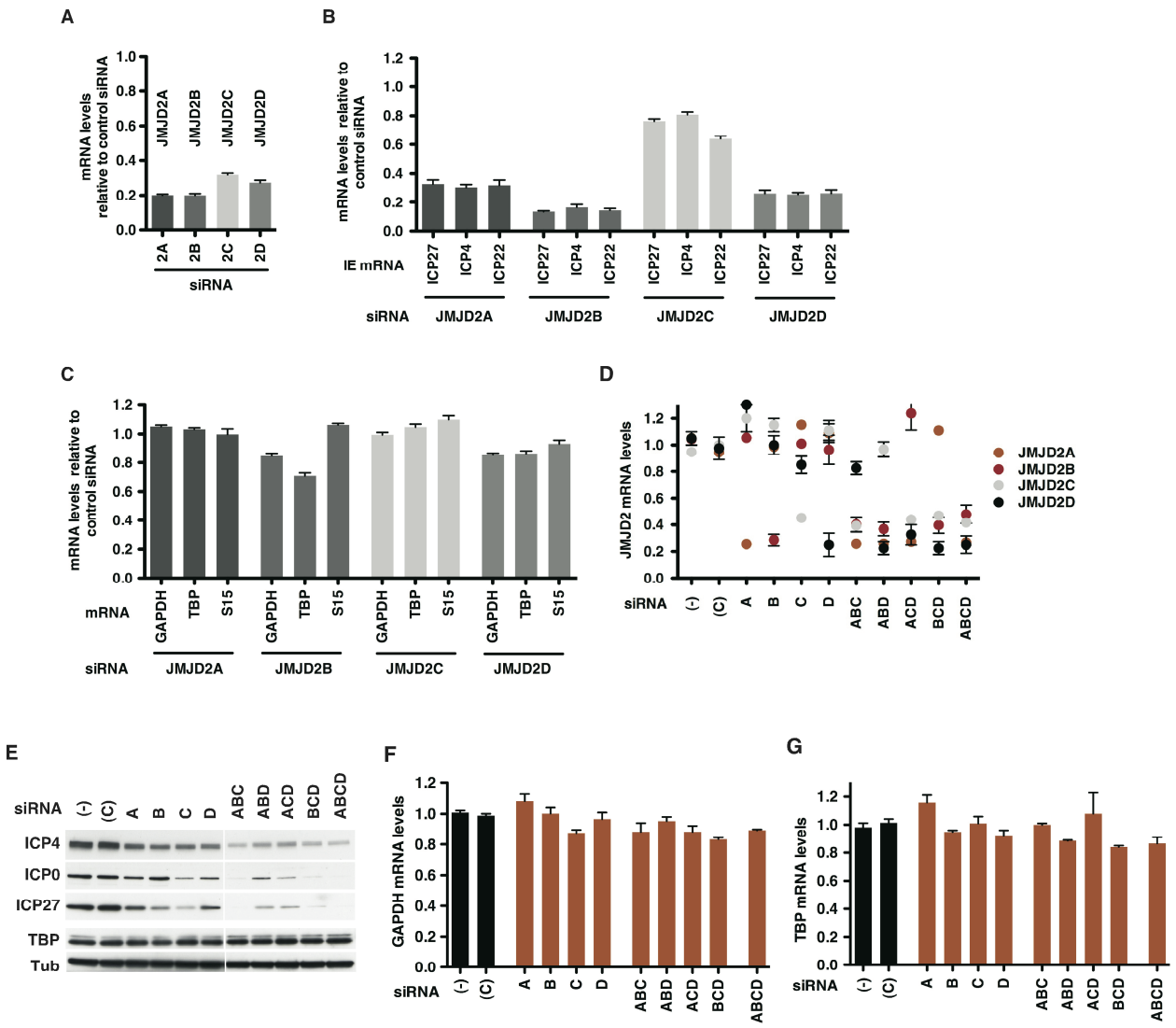

Fig. S1. Depletion of JMJD2 members resulted in decreased HSV-1 IE mRNAs.

(**A-C**) MRC-5 cells were transfected with 5 nM of individual siRNA to JMJD2A, B, C, or D, followed by infection with HSV-1 (0.1 pfu/cell) for 2h. The mRNA levels of the JMJD2 family members (**Panel A**), HSV-1 viral IE genes (ICP 27, ICP4 ICP22; **Panel B**), and cellular controls (GAPDH, TBP, S15; **Panel C**) are expressed as ratios to the levels in cells transfected with control siRNA. (**D-G**) HeLa cells were transfected with 1 □M of control, individual JMJD2, or

combinations of JMJD2s siRNAs, followed by infection with HSV-1 (0.1 pfu/cell) for 2h. (**A**) JMJD2 mRNA levels were determined by qRT-PCR. (**B**) mRNA levels (**see Fig. 1**) and protein levels of the viral IE and cellular controls were determined by Western blot. (**F-G**) mRNA levels of cellular controls GAPDH and TBP in cells depleted for individual and combinations of JMJD2 proteins. (-) no siRNA; (C), control siRNA.

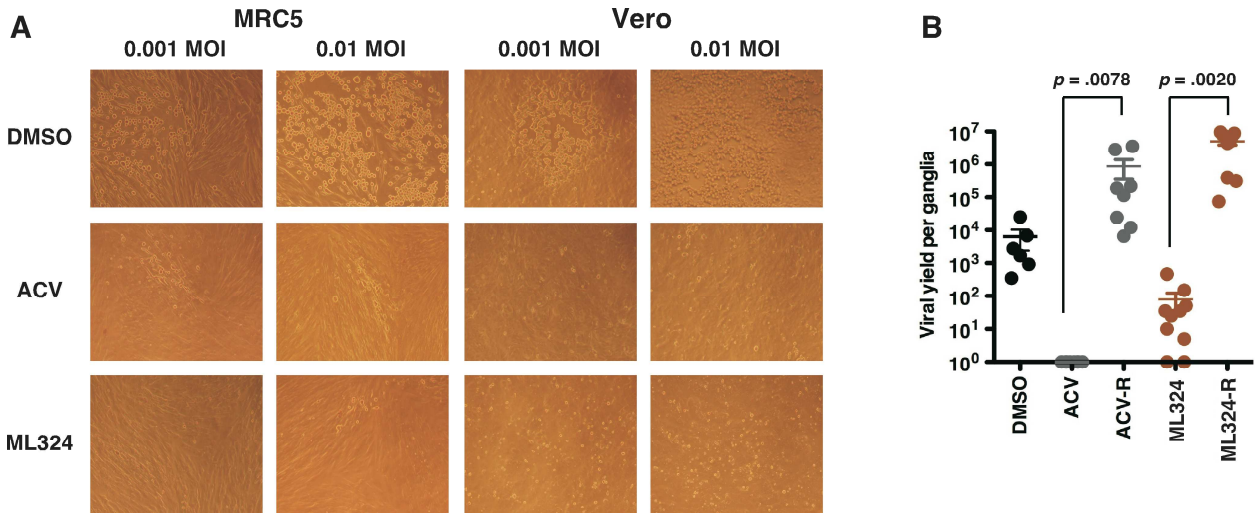

Fig. S2. ML324-mediated inhibition of HSV lytic infection and reactivation from latency. (A) Representative fields of MRC-5 and Vero cells infected with HSV-1 for 12 hrs followed by addition of DMSO, ACV (100 μM) or **ML324** (50 μM) for 48 hrs. (B) Latently infected ganglia were explanted in the presence of DMSO, ACV (100 μM), or **ML324** (50 μM) for 48 hrs. Viral yields were determined from one half of each ganglia at 48 hrs (DMSO, ACV, **ML324**) and from the other half of each ganglia after drug reversal for an additional 72 hrs (ACV-R, **ML324**-R) [Wilcoxon matched pairs signed rank test, ACV vs ACV-R $n = 8$, ML324 vs ML324-R $n = 10$].

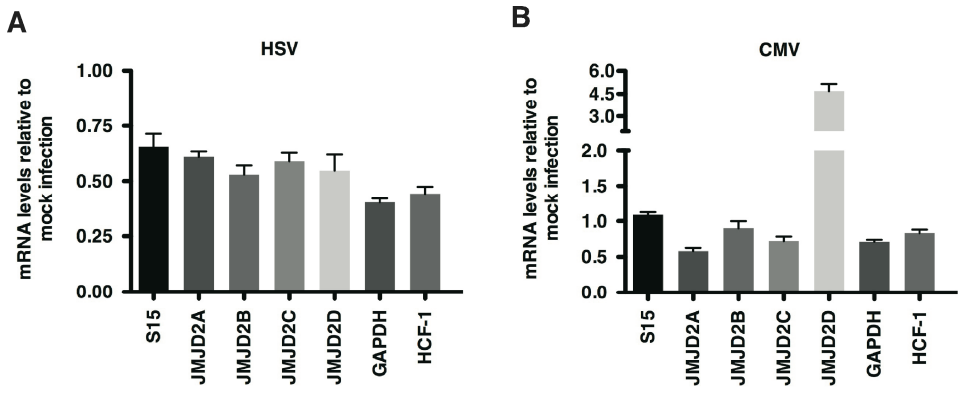

Fig. S3. Selective induction of JMJD2D transcription upon infection with hCMV.

HFF cells were mock-infected or infected with HSV-1 (10 pfu/cell, **Panel A**) or hCMV (0.2 pfu/cell, **Panel B**) for 2.5 hrs. The levels of JMJD2, HCF-1, and cellular control mRNAs are expressed relative to the levels in mock-infected cells. The data shown is representative of two independent experiments.

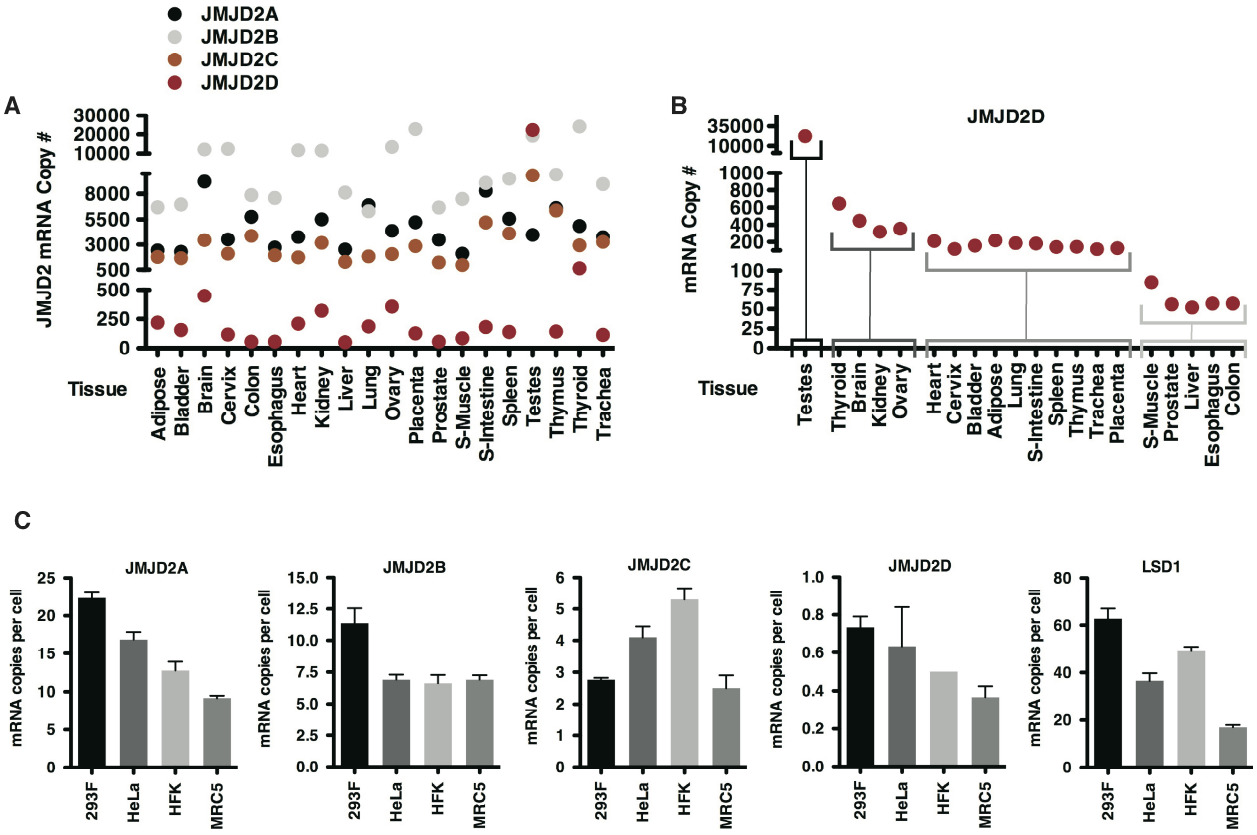

Fig. S4. Levels of JMJD2 mRNAs in selected tissues and cell types.

The mRNA levels of JMJD2 family members were determined from equal amounts of RNA from the indicated tissues (**A-B**) or cultured cells (**C**). Titrations of plasmid DNAs containing the JMJD2 genes were used as qPCR standards. The results are graphed as the absolute copy number per unit of RNA (tissue samples) or the absolute copy number per cell (cultured cells). JMJD2 mRNA copy numbers in tissues were determined using the First Choice Total RNA Survey Panel (Ambion). (**B**) Tissue levels of JMJD2D mRNAs are arranged in clusters according to the absolute level for reference.

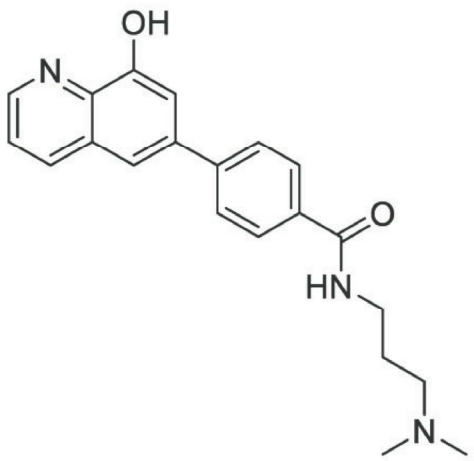

Fig. S5. Structure and characteristics of ML324.

N-(3-(dimethylamino)propyl)-4-(8-hydroxyquinolin-6-yl)benzamide (**1**). LC-MS: rt (min) = 3.033; ^{1}H NMR (400 MHz, DMSO-d_6) δ 1.84-1.98 (m, 2 H), 2.79 (s, 3 H), 2.80 (s, 3 H), 3.12 (ddd, *J* =10.2 Hz, 5.4 Hz and 5.2 Hz, 2 H), 3.37 (q, 2 H), 7.50 (s, 1 H), 7.66 (dd, *J* = 8.2 Hz and 4.3 Hz, 1 H), 7.84 (s, 1 H), 7.88 - 7.94 (m, 2 H), 7.96 - 8.02 (m, 2 H), 8.50 (d, *J* = 8.2 Hz, 1 H), 8.71 (t, *J* = 5.6 Hz, 1 H), 8.90 (d, *J* = 4.1 Hz, 1 H), 9.34 (brs, 1 H); HRMS (ESI) *m*/*z* $(M+H)^+$ $C_{21}H_{24}N_3O_2$, 350.1867; found 350.1863.

PRIMERS

TARGET	*SEQUENCE*
	ChIP
ICP0	TAACTTATACCCCACGCCTTTC
(-315 to -20)	TCCGGGTATGGTAATGAGTTTC
ICP0 (R1)	CGCGGGTCGCTCAATGAAC
Promoter Distal (-354 to -170)	GCCCGGCCCCCGATT
ICP0 (R15)	CCCTGGCCCGACAGTCT
Promoter Proximal (-15 to +186)	CAGGCCGGCGGGTACTC
ICP27 (P1)	GTCCCGTTACCAAGACCAAC -235
Promoter Distal (-235 to -102)	GCACAGACAAGGACCAATCA -102
	Ottosen et al., (2006) Virology 345:468.
ICP4	TAGCATGCGGAACGGAAGC
(-304 to -248)	CGCATGGCATCTCATTACCG
	Cliffe & Knipe, (2008) J Virology 82:12030.
RPL30	CAAGGCAAAGCGAAATTGGT
	GCCCGTTCAGTCTCTTCGATT
	Abcam ab74244; ab83296
SATa	AAGGTCAATGGCAGAAAAGAA
	CAACGAAGGCCACAAGATGTC
	Abcam ab83620; ab83621
p107	GGCAGACGGTGGATGACAACACG
(-56 to +105)	TCAGCGTGGGGCTTGTCCTCGAAC
	Takahashi et al., (2000) Genes Dev. 14:804.
GAPDH	TACTAGCGGTTTTACGGGCG
(-118 to +46)	TCGAACAGGAGGAGCAGAGAGCGA
	Nested PCR
ICP4	GCGAGCAGCCCCAGAAACTC
	ACGACGATAACCCCCACCC
ICP4-Nested	GGACAGCAGCAGCACGCC
	ATCCCCGACCCCGAGGACG
ICP27	CCCCAGGACCCCATTATCG
	TTCTCTCCGACCCCGACACCAAGG
ICP27-Nested	GCTGGATAACCTCGCCACG
	CAGAATGACAAACACGAAGGATGC
	qRT-PCR
ICP27	GCATCCTTCGTGTTTGTCATTCTG
	GCATCTTCTCTCCGACCCCG
ICP4	TGCTGCTGCTGTCCACGC
	CGGTGTTGACCACGATGAGCC
ICP22	TTTGGGGAGTTTGACTGGAC
	CAGACACTTGCGGTCTCTG
	Ottosen et al., (2006) Virology 345:468.
S15	TTCCGCAAGTTCACCTACC
	CGGGCCGGCCATGCTTTACG
UL32-ORF	TCCAACTACTCGTTCCTGGCG
	GTGAGCGACGGCTGCGTG
UL47-ORF	CGTCTCCCATCAGCAGTTTCC
	GACCCCGCCTTTCTTCTCAAG
GAPDH	TTCGACAGTCAGCCGCATCTTCTT
	CAGGCGCCCAATACGACCAAATC
	Cliffe & Knipe, (2008) J Virology 82:12030.
Sp1	TCAGAACCCACAAGCCCAAAC
	TGCCAGCAGGAATGGAAGC
TBP	TGACCCCCATCACTCCTGC
	CGTGGTTCGTGGCTCTCTTATC

TARGET	*SEQUENCE*
	RT-PCR-(continued)
JMJD2A	GAAGCCACGAGCATCCTATGA
	GCGGAACTCTCGAACAGTCA
	PrimerBank ID 98986458b2
JMJD2B	ACTTCAACAAATACGTGGCCTAC
	CGATGTCATCATACGTCTGCC
	PrimerBank ID 193083181b1
JMJD2C	GATGAATGGAACATAGCTCGCC
	GGTGTGCCATGCAAACGTG
	PrimerBank ID 226442896b3
JMJD2D	GGGCAGGGGTGTTTACTCAAT
	TTGCCAAATGGCGATACTCCC
	PrimerBank ID 396533316b1
LSD1	TGACCGGATGACTTCTCAAGA
	GTTGGAGAGTAGCCTCAAATGTC
	PrimerBank ID 226437585b1
IE72	CCTAGTGTGGATGACCTA
	GTGACACCAGAGAATCAG
US3	GCCCCTGAATGTGGTGGTATC
	TTCTTGGTGAAGTTGCCCGAC
UL37	GACGAAGTCCGATGAGGAGGATG
	TGGGACACTGGGCGTTGTTG
	siRNA-resistance
2B	CGGGCCGGAGAGGGGCAGGCgCCeagCACgTTeTCCAAATTGAAG
	CTTCAATTTGGAgAAcGTGctgGGeGCCTGCCCCTCTCCGGCCCG
2C	CCAGATAGCAATGAAGAGgGAGGAtATaTACACgeTAGATGAAGAGTTACCCAAGAG
	CTCTTGGGTAACTCTTCATCTAgeGTGTAtATaTCCTCeCTCTTCATTGCTATCTGG
2D	GGAGCGAAAATACTGGAAGAAtaGgATbTAcAATTCACCGATTTATGGTGCTGACATCAGTGGC
	GCCACTGATGTCAGCACCATAAATCGGTGAATTgTAtATeCtaTTCTTCCAGTATTTTCGCTCC

Primer Bank References

Spandidos et al.,(2010) Nucl. Acids Res. 38:792.
Spandidos et al., (2008) BMC Genomics 9:633.
Wang and Seed, (2003) Nucleic Acids Research 31(24):1.

ANTIBODIES

ICP0	Goodwin Institute for Cancer Research #1112
ICP4	Goodwin Institute for Cancer Research #1114
ICP27	Goodwin Institute for Cancer Research #1113
UL29	Gift of W. Ruyechan, University of New York, Buffalo
TBP	Santa Cruz sc-273
Tubulin	Santa Cru sc-9104
Flag	Sigma Anti-FLAG M2 Affinity Gel A2220
	Sigma Anti-FLAG M2- peroxidase conjugate A8592
HA	Roche Anti-HA-Peroxidase clone 3F10
IgG	Millipore 12-370
H3K9-me3	Abcam ab8898
H3	Abcam ab1791
JMJD2A	Bethyl A300-861A
JMJD2B	Bethyl A301-477A
JMJD2D	Santa Cruz sc-13370
HCF-1	Kristie et al., (1995) J Biol. Chem. 270: 4387.
V5-Agarose	Sigma Anti-V5 Agarose Affinity Gel clone V5-10 #A7345
V5-Peroxidase	Anti-V5 peroxidase conjugate clone V5-10 #V2260

siRNAs

	Dharmacon Smartpool
JMJD2A	M-004292-01
JMJD2B	M-004290-01
JMJD2C	M-004293-01
JMJD2D	M-020709-00
Non-Targeting Control	D-001206-14-15
	Individual siRNAs
JMJD2A	Dharmacon D-004292-01
JMJD2B	Dharmacon D-004290-07
JMJD2C	Dharmacon D-004293-04
JMJD2D	Qiagen SI4335198
HCF-1	Qiagen SI04332755
LSD1	Qiagen SI02781177
Non-Targeting Control	Qiagen 1027280

Table S1. Antibodies and primers.

Primer sequences for ChIP qPCR, qRT-PCR, nested PCR, and for construction of siRNA-resistant JMJD2 expression clones. Where appropriate, coordinates are given relative to the site of transcription initiation. Antibodies and sources are listed.